Lattice Monte Carlo Study of the Harmonic Oscillator in the Path Integral Formulation

DESY Summer Student Programme, 2012

Aleksandra Słapik
University of Silesia, Poland

Willian M. Serenone
University of São Paulo, Brazil

Supervisor:
Karl Jansen

31st of August 2012

Abstract

The Path Integral is a mathematical entity used on Gauge Field Theories such as Quantum Electrodynamics (QED) and Quantum Chromodynamics (QCD). For most physical systems it is impossible to evaluate the path integral analytically. In our project we study the method of evaluating the path integral numerically on the simpler case of a path integral formulation of non-relativistic quantum mechanics. We use the Metropolis algorithm to do this evaluation on the test case of the harmonic oscillator, which has an analytical solution.

Contents

1 Introduction

1.1 The Path Integral Formulation of Non-Relativistic Quantum Mechanics

To arrive at the path integral formulation of quantum mechanics we consider the problem of calculating the probability of a particle leaving a position q_I and arriving at a position q_F under the action of a potential $V(q)$ in a time T. We will follow the steps first made by Dirac to arrive at the path integral formalism [1]. The probability is given by $\langle q_F|e^{-iHT}|q_I\rangle$ (we will be adopting natural units for all our calculations). We divide the time T in N steps of size δt such as $N\delta t = T$. This will result in

$$\langle q_F|e^{-iHT}|q_I\rangle = \langle q_F|e^{-iH\delta t}e^{-iH\delta t}\dots e^{-iH\delta t}|q_I\rangle\,. \tag{1}$$

We insert then between each exponential the completeness relation $\int dq|q\rangle\langle q| = 1$

$$\langle q_F|e^{-iHT}|q_I\rangle = \left(\prod_{i=1}^{N-1}\int dq_i\right)\langle q_F|e^{-iH\delta t}|q_{N-1}\rangle\langle q_{N-1}|e^{-iH\delta t}\dots e^{-iH\delta t}|q_1\rangle\langle q_1|q_I\rangle\,. \tag{2}$$

The interpretation is that we divide our time axis in N time slices and then compute the probability amplitude for the particle leaving a position q_i at time t_i and reaching the position q_{i+1} at time t_{i+1}. The next step is to multiply these amplitudes to obtain the probability amplitude for the particle leaving q_I arrive at q_F in a time T through a specific path. We repeat this for all possible paths and sum the amplitudes for each path to obtain the total probability amplitude $\langle q_F|e^{-iHT}|q_I\rangle$. We proceed then to compute $\langle q_{i+1}|e^{-iH\delta t}|q_i\rangle$ using the completeness relation for momentum base ($\int dp|p\rangle\langle p| = 2\pi$)

$$\langle q_{i+1}|e^{-iH\delta t}|q_i\rangle = \int\frac{dp}{2\pi}\langle q_{i+1}|e^{-iH\delta t}|p\rangle\langle p|q_i\rangle\,. \tag{3}$$

The Hamiltonian is written as $H = p^2/(2m) + V(q)$. We then write the exponential as a power series of the operator H and use the relations $\langle q|p|\psi\rangle = \dot{\psi}(x)$ and $\langle q|p\rangle = e^{ipq}$. The end result is the Gaussian integral

$$\langle q_{i+1}|e^{-iH\delta t}|q_i\rangle = \frac{e^{-i\delta tV(q_{i+1})}}{2\pi}\int dp\exp\left[-i\delta t\frac{p^2}{2m} + ip(q_{i+1}-q_i)\right]\,,$$

which can easily be evaluated by completing squares

$$\langle q_{i+1}|e^{-iH\delta t}|q_i\rangle = \left(\frac{-im}{2\pi\delta t}\right)^{1/2}\exp\left\{i\delta t\left[\left(\frac{q_{i+1}-q_i}{\delta t}\right)^2 - V(q_{i+1})\right]\right\}\,. \tag{4}$$

Now we have the amplitude for a particle leaving the position q_i to arrive in the position q_{i+1} in a time δt. We can insert eq. (4) into eq. (3) to obtain the total probability amplitude

$$\langle q_F|e^{-iHT}|q_I\rangle = \left(\frac{-im}{2\pi\delta t}\right)^{\frac{N-1}{2}}\left(\prod_{i=1}^{N-1}\int dq_i\right)\exp\left[i\delta t\sum_{j=0}^{N-1}\left(\frac{q_{j+1}-q_j}{\delta t}\right)^2 - V(q_{j+1})\right]\,. \tag{5}$$

But time is not a discrete quantity. It means we must consider now the continuum limit, making δt increasingly small (and conversely N increasingly large). On this limit we define

$$\left(\frac{-im}{2\pi\delta t}\right)^{\frac{N-1}{2}} \left(\prod_{i=1}^{N-1}\int dq_i\right) \to \int \mathcal{D}[q(t)],$$
$$\frac{q_{j+1}-q_j}{\delta t} \to \dot{q},$$
$$\delta t \sum_{j=0}^{N-1} \to \int dt,$$

to obtain the final expression for the probability amplitude

$$\langle q_F|e^{-iHT}|q_I\rangle = \int \mathcal{D}[q(t)] \exp\left[i\int dt \frac{m\dot{q}^2}{2} - V(q)\right].$$

We can see that the integral on the exponential is just the definition of the action. Finally, we rewrite the probability amplitude as

$$\langle q_F|e^{-iHT}|q_I\rangle = \int \mathcal{D}[q(t)] e^{iS[q(t)]}. \tag{6}$$

1.2 The Quantum Mechanics Connection with Statistical Mechanics

The path integral has an analytical solution only on some simple cases, and then on the way it appears in eq. (6) that it is not a good way to evalluate it numerically. Our aim will be to relate the path integral with the partition function on statistical mechanics and use the Metropolis algorithm to make a Monte Carlo simulation to evaluate the path integral.

The first step is to transform from the Minkowski time to the Euclidean time, that means $t \to -it$. The names comes because when we do this transformation the Minkowski metric becomes the Euclidean metric. The second step is to step back from eq. (6) to eq. (5), since we will be evaluating this integral on computers. The result of these transformation will be

$$Z_{FI} = \left(\frac{-im}{2\pi\delta t}\right)^{\frac{N-1}{2}} \left(\prod_{i=1}^{N-1}\int dq_i\right) \exp\left[-\delta t \sum_{j=0}^{N-1}\left(\frac{q_{j+1}-q_j}{\delta t}\right)^2 + V(q_{j+1})\right]. \tag{7}$$

Where $Z_{FI} = \langle q_F|e^{-iHT}|q_I\rangle$. Notice that on the Euclidean time the Lagrangian is the Hamiltonian on Minkowski time. Also, the integral is now extremely similar to the partition function on statistical mechanics. This means we can use statistic mechanics methods to evaluate the integral and to obtain other measurable quantities such as the ground state energy of the system.

Before the proceeding, we define the average of an operator $\hat{A}$ as

$$\langle\hat{A}\rangle = \mathrm{Tr}[e^{-H^T}\hat{A}]/Z = \frac{\int\langle x|e^{-H^T}\hat{A}|x\rangle\, dx}{Z}, \tag{8}$$

where Z is defined by (see ref. [2])

$$Z = \mathrm{Tr}\left[Z_{FI}\right] = \int dx \langle x|e^{-HT}|x\rangle = \int dq_I dq_F \delta(q_F - q_I) Z_{FI}\,. \tag{9}$$

We first remark that Z is just Z_{FI} with $F = I$ and integrated over all possible values for intial (and final) points and thus it is a path integral also. We can use this information from eq. (9) to notice that eq. (8) is also a path integral. Alternatively, we can use the same procedure exposed on section (1.1). The end result is that eq. (8) can be written as

$$\langle \hat{A} \rangle = \frac{\left(\prod_{i=0}^{N} \int dx_i\right) A(x_1, x_2, \ldots, x_n) e^{-S[x(t)]}}{\left(\prod_{i=0}^{N} \int dq_i\right) e^{-S[x(t)]}} \tag{10}$$

If our system has M (M may be infinity) discrete energy levels, we can insert the completeness relation $\sum_{n=1}^{M} |n\rangle\langle n| = 1$ on (8) and taking the limit $T \to \infty$ we find

$$\langle \hat{A} \rangle = \langle 0|\hat{A}|0\rangle\,. \tag{11}$$

This way, we can isolate the ground energy level by observing the value of the Hamiltonian behavior at large T, which means evaluating the path integral at eq. (10) for large T. For our calculations we use the virial theorem

$$\langle m\dot{x}^2 \rangle = \langle x V'(x) \rangle\,, \tag{12}$$

that allow us to write eq. (10) as

$$E_0 = \lim_{T\to\infty} \langle \hat{H} \rangle = \frac{\left(\prod_{i=0}^{N} \int dx_i \left[x_i V'(x_i)/2 + V(x_i)\right] e^{-S[x(t)]}\right)}{\left(\prod_{i=0}^{N} \int dx_i\right) e^{-S[x(t)]}}. \tag{13}$$

For calculation of the first excited state we need to introduce the connected n-point propagator functions

$$\Gamma_c^{(n)} = \prod_{i=1}^{n} \frac{\partial}{\partial J_i} \ln\left[Z(J)\right]\Big|_{J=0}\,, \tag{14}$$

where J is just a complex number and $Z(J)$ is modificate version of eq. (9)

$$Z(J) = \mathrm{Tr}\left[\exp\left(-HT + \sum_{k=1}^{n} x_k J_k\right)\right]\,. \tag{15}$$

Notice that $\partial J_k / \partial J_i = \delta_{ik}$.

If we choose $n = 2$ to evaluate eq. (14) and use eq. (8) we arrive at

$$\Gamma_c^{(2)} = \langle x(0)x(\tau)\rangle - \langle x(0)\rangle\langle x(\tau)\rangle\,.$$

We take then the limit of $T \to \infty$, which allow us to use eq. (11) and rewrite the expression above as

$$\Gamma_c^{(2)} = \langle 0|x(0)x(\tau)|0\rangle - \langle 0|x(0)|0\rangle\langle 0|x(\tau)|0\rangle\,.$$

By inserting the completeness relation $\sum_{n=0} |n\rangle\langle n| = 1$ among $x(0)$ and $x(\tau)$ we find

$$\Gamma_c^{(2)} = \sum_{n\neq 0} \langle 0|x(0)|n\rangle\langle n|x(\tau)|0\rangle \,. \tag{16}$$

We must highlight that the operators $x(\tau)$ are in the Heisenberg representation. This means there is a time dependence on the equation above. We can extract it by transforming to the Schrödinger representation through the relation $x(\tau)_H = e^{-HT} x_S e^{HT}$. We arrive then at

$$\Gamma_c^{(2)} = \sum_{n\neq 0} |\langle 0|x|n\rangle|^2 \, e^{-(E_n - E_0)\tau} \,. \tag{17}$$

If we consider the limit of large τ we actually manage to isolate the difference between the ground state and the first excited state

$$\Gamma_c^{(2)} = |\langle 0|x|1\rangle|^2 \, e^{-(E_1 - E_0)\tau} \,. \tag{18}$$

This opens possibilities for two methods of determining E_1. The first consists of plotting the results for $\Gamma_c^{(2)}$ as function of τ and then fit on these points the function eq. (18). The other possibility is to compute the quantity $\Gamma_c^{(2)}(\tau + \Delta\tau)/\Gamma_c^{(2)}(\tau)$. This will essentially remove the constant accompanying the exponential in eq. (18) and then we finally arrive to the expression for E_1

$$E_1 = E_0 - \frac{1}{\Delta\tau} \ln \left[\frac{\Gamma_c^{(2)}(\tau + \Delta\tau)}{\Gamma_c^{(2)}(\tau)} \right] . \tag{19}$$

1.3 Analytical Solution of the Harmonic Oscillator with Path Integrals

The harmonic oscillator is one of the few systems which have an analytical solution, which makes it an excellent system for testing our algorithm. Its solution may be found on ref. [2] for the case of a particle of unitary mass. Here we will state these results and generalise them.

The action used on ref. [2] is given by

$$S = a \sum_{j=1}^{N} \left(\frac{x_{j+1} - x_j}{a} \right)^2 + \frac{\mu^2 x_j^2}{2} \,. \tag{20}$$

and the average of the operator x^2 is

$$\langle x^2 \rangle = \frac{1}{2\mu\sqrt{1 + \frac{a^2\mu^2}{4}}} \left(\frac{1 + R^N}{1 - R^N} \right) , \tag{21}$$

where R is given by

$$R = 1 + \frac{a^2\mu^2}{2} - a\mu\sqrt{1 + \frac{a^2\mu^2}{4}} \,. \tag{22}$$

The ref. [2] also gives the expression for the correlation functions $\langle x_{i+j} x_i \rangle$

$$\langle x_{i+j} x_i \rangle = \frac{R^j + R^{N-j}}{2(1 - R^N)\mu\sqrt{1 + \frac{a^2\mu^2}{4}}} \tag{23}$$

We use the value of $\langle x^2 \rangle$ to calculate the ground energy through the virial theorem [eq. (12)]

$$E_0 = \mu^2 \langle x^2 \rangle = \frac{\mu}{2\sqrt{1 + \frac{a^2\mu^2}{4}}} \left(\frac{1 + R^N}{1 - R^N} \right) . \tag{24}$$

We can use as well the correlation functions to calculate E_1

$$E_1 = E_0 - \frac{1}{a} \ln \left[\frac{R^{j+1} - R^{N-j-1}}{R^j - R^{N-j}} \right] \tag{25}$$

These calculations were all done with the mass set equal unity. However we are interested in the action

$$S = a \sum_{j=1}^{N} m \left(\frac{x_{j+1} - x_j}{a} \right)^2 + \frac{\mu^2 x_j^2}{2} . \tag{26}$$

To solve our problem, we rescale x: $x \to x/\sqrt{m}$. The action then becomes

$$S = a \sum_{j=1}^{N} \left(\frac{x_{j+1} - x_j}{a} \right)^2 + \frac{\mu^2 x_j^2}{2m} . \tag{27}$$

This means that on every expression it will be necessary to make the replacement $\mu \to \mu/\sqrt{m}$ as well. We find then

$$\langle x^2 \rangle = \frac{1}{2\mu\sqrt{m + \frac{a^2\mu^2}{4}}} \left(\frac{1 + R^N}{1 - R^N} \right) \tag{28}$$

$$R = 1 + \frac{a^2\mu^2}{2m} - a\mu \sqrt{\frac{1}{m} + \frac{a^2\mu^2}{4m^2}} \tag{29}$$

$$\langle x_{i+j} x_i \rangle = \frac{R^j + R^{N-j}}{2(1 - R^N)\mu\sqrt{m + \frac{a^2\mu^2}{4}}} \tag{30}$$

$$E_0 = \frac{\mu}{2\sqrt{m + \frac{a^2\mu^2}{4}}} \left(\frac{1 + R^N}{1 - R^N} \right) = \mu^2 \langle x^2 \rangle . \tag{31}$$

Notice that the expression for E_1 is the same as in eq. (25), but with the definition of R given in eq. (29).

2 Numerical Approach to Evaluate Path Integrals

As we have already discussed, often no analytical approach is possible to solve the path integral. For this reason we are forced to use numerical methods and introduce numerical approximations. To calculate path integrals we use Monte Carlo method, but not in its ordinary way. We apply Metropolis algorithm to generate random paths between initial and final position of the particle. The difference is that instead of random sampling we base on importance sampling, which is sampling from a proposal distribution. Let us explain the main idea of our computations.

The aim of using Monte Carlo method is to approximate any expectation by the sample mean of a function of simulated random variables. Considering a random variable X with probability density function $f_X(x)$ on a set of values A, the expected value of any function g in dependence of X can be expressed by the following equation

$$\mathbb{E}(g(X)) = \sum_{x \in A} g(x) f(x) \tag{32}$$

if X is discrete, and

$$\mathbb{E}(g(X)) = \int_{x \in A} g(x) f(x) dx \tag{33}$$

if X is continuous. After taking a n-sample of X random variables we compute the mean of $g(x)$ over the sample

$$\bar{g_n}(x) = \frac{1}{n} \sum_{i=1}^{n} g(x_i) \tag{34}$$

which is the Monte Carlo estimate. According to the laws of large numbers, an obtained average should be close to the expected value. In our project we used Monte Carlo method to approximate a definite integral, which can be described by the formula

$$\int f(x) \mathcal{D}x \approx \sum f(x_i) \cdot \Delta x_i, \tag{35}$$

where x_i are the elements of our space.

The most important matter is how to choose these x_i points to get the best approximation in the most optimal way. There are two possible solutions. We can choose the x_i random points according to a uniform distribution over the whole space - this is what we call random sampling. But if the given space is large, a huge number of points is needed to cover it and this quickly becomes problematic. In such case not all regions in our space contribute and, therefore a lot of integration points will be wasted on unimportant areas.

This is the reason of using importance sampling - generate x_i points, which are not totally random, but more densely distributed in dominant regions of the given space. The idea is to choose a good distribution from which one simulates random variables.

Let us now introduce the realization of importance sampling concerning path integrals. We consider a Boltzmann distribution with the action S treated as a factor, thus, probability function can be interpreted according to the following

$$P(x) \sim \exp(-S). \tag{36}$$

The expected value of any observable A is given by the expression

$$\langle A \rangle = \frac{1}{Z} \int A(x) \exp[-S(x)] \mathcal{D}x, \tag{37}$$

where

$$Z = \int \exp\left[-S(x)\right]\mathcal{D}x \tag{38}$$

is the partition function. We need to find the way of generating random points x_i with the distribution

$$P(x) = \frac{\exp\left[-S(x)\right]}{\int \exp\left[-S(x)\right]\mathcal{D}x}, \tag{39}$$

which will lead us to obtain the Monte Carlo estimate $\bar{A}$ of the expectation value $\langle A \rangle$ as shown below:

$$\langle A \rangle = \frac{1}{N}\sum_{i=1}^{N} A(x_i). \tag{40}$$

2.1 Metropolis Algorithm

In this section we are going to present the main concept of the Metropolis algorithm. The algorithm was named after Nicholas Metropolis who was one of the authors of the 1953 paper *Equation of State Calculations by Fast Computing Machine*, which first proposed the algorithm for the specific case of the Boltzmann distribution. The most important attribute of the algorithm is the use of importance sampling.

Suppose that $S(x)$ is the action of the given system, Δ_x is an algorithm parameter and x is a set of points representing coordinates in quantum mechanics and fields fields in quantum field theory. Assume that N is the number of points on our time lattice and therefore number of the particle path's coordinates as well. Let the following scheme explain the mechanism of Metropolis algorithm.

1. Generate any random path $x = (x_1, x_2, \ldots x_N)$ between initial and final position of the particle. Let it be called *initial path.*

2. Choose the random point x_i' with uniform probability within the interval

$$[x_i - \Delta_x, x_i + \Delta_x].$$

3. Replace point x_i with new value x_i' and calculate the difference in action

$$\Delta S(x_i', x_i) := S(x_i') - S(x_i).$$

4. If $\Delta S(x_i', x_i) < 0$, then accept x_i point and change *initial path.* Apply algorithm for the next point of *initial path.*

5. If $\Delta S(x_i', x_i) \geq 0$, then generate random number r within the $[0, 1]$.

   - If $\exp\left[-\Delta S(x_i', x_i)\right] > r$, then accept x_i point and change *initial path.* Apply algorithm for the next point of *initial path.*
   - Otherwise, reject x_i' and apply algorithm for the next point of *initial path.*

To minimize probability of correlation between following points x_i, what will be discussed later, the Metropolis algorithm should be repeated severals times. According to [2] we introduce the $\bar{n}$ parameter, which is responsible for number of algorithmic iterations for every x_i point.

In order to get the proper sample of path's points x_i we have to generate several trajectories using given algorithm. Statistical calculation can be done only after thermalization point is reached. It means the point, when we can see that obtained configuration is close to the desired equilibrium distribution $P(x)$. When the system accomplished thermalization state, obtained values can be used to compute the Monte Carlo estimate for expected value. In the figure below 1a thermalization of x_i^2 values can be easily seen.

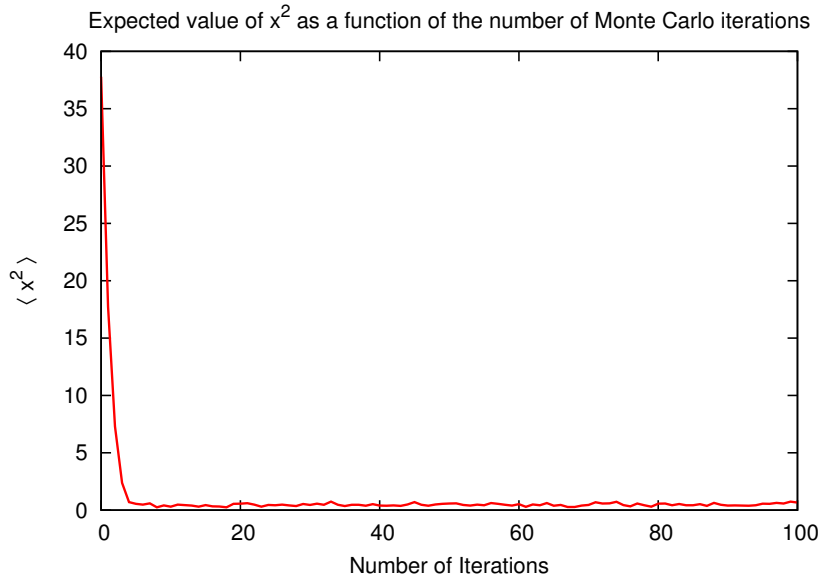

Figure 1: Thermalization of x_i^2 values occurs rapidly after five iterations. Axis: x - number of the path, y - value of x_i^2 for i given path.

2.2 Error Effects in the System

Computing errors of expection values in Monte Carlo simulations base on independent measurements, what unfotunatelly is difficult in practise. There can appear some systematic effects due to the pseudo-random mechanism and, more importantly, due to the fact that the new coordinate depends of the old one. We observe correlation between different paths and its impact on expectation. Therefore there are some statistical dependencies between different configurations. To measure how variables $X_i(s)$ and $X_j(s')$ are dependent on each other in two different points s, s' we can use a correlation function

$$C_{ij}(s, s') = corr(X_i(s), X_j(s')), \tag{41}$$

where $corr$ is given by the expression

$$corr(X, Y) = \rho_{X,Y} = \frac{E[(X - \bar{X})(Y - \bar{Y})]}{\sigma_X \sigma_Y}. \tag{42}$$

Symbols $\bar{X}$ and $\bar{Y}$ are expected values of the variables, σ_X and σ_Y standard deviations and finally E stands for expected value of X and Y. Basically, correlation can assume values from $[0, 1]$ interval and it describes how similar two functions or sequences are. If correlation value is equal to zero, we expect no connection between the data. Otherwise, if value is equal to 1, functions or sequences are exacly the same.

In order to truly understand obtained results we have to investigate correlation (more specifically autocorrelation) between paths generated by Metropolis algorithm and take it into account in error analysis. Autocorrelation function for our algorithm is claimed to have an exponential decay of the form

$$C(t) \sim e^{\frac{-t}{\tau_{ac}}}. \tag{43}$$

The τ_{ac} parameter is called autocorrelation time and plays the main role in statistical results.

In more strict mathematical sense, algorithm which we use to generate the configurations for each path is a Markov process. The problem with Metropolis algorithm is that in Monte Carlo Markov Chain random walk following samples will usually be highly correlated, what can be seen in fig. 2a. Generated path is very similar to previous one and in the end it effects in our statistical aproach. The true error is underestimated, because the error does not decrease with the square root of the number of samples if the samples are not independent of each other.

To avoid described situation we introduce several parameters according to the suggestions made in [2]. We have $\bar{n}$ value for repeating Metropolis algorithm for each x_i point. Thus we let the algorithm wander around initial point for some time, long enough to change its position and be no longer closely related to the initial point. What we apply as well is M value, which is the number of paths that are skipped while calculating expected value.

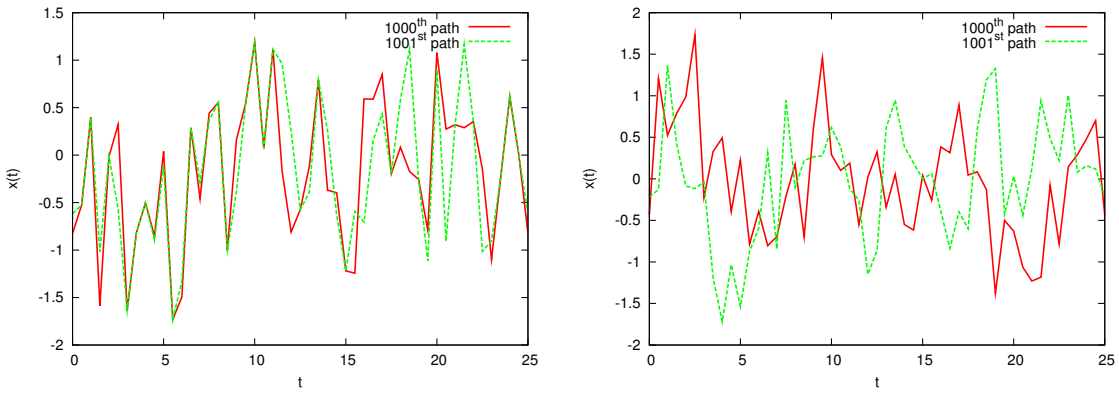

Figure 2: Two subsequent paths, total number of paths: 10^5. Left: $\bar{n} = 1$. Right: $\bar{n} = 5$.

To verify mentioned treatments one can pick some observable and check how closely it is correlated with the value of the previous state. It is typically found that the correlation of an observable with its initial value decreases exponentially with the number of steps made, which suggests that the state of the system itself decorrelates exponentially with the number of algorithm's iterations. Consequently, if one let the system wander around for a few system autocorrelation times between measuring samples, the measurements have a good chance of being statistically independent of each other.

3 Results for the Harmonic Oscillator

3.1 The Energy of the Ground State

We aim to compute the observables for the harmonic oscillator. Our program calculates the expected value for the square of the position $\langle x^2 \rangle$, since through the virial theorem [eq. (12)], $E_0 = \mu^2 \langle x^2 \rangle$. The parameters chosen for our simulations was $m = 0.5$, $\mu^2 = 2$, $\Delta = 2\sqrt{a}$ and $\overline{n} = 10$. For these parameters we have on the continuum limit $E_0 = 1.0$ and that is the value we hope to find numerically.

On all cases we consider the equilibrium to be reached after 100 Monte Carlo iterations. We also take measurements for $M = 5$, that is every each 5 Monte Carlo iterations. This is to try to enforce that the quantities measured are completely decorrelated from each other. Since we are interested on the continuum limit, we run our simulation with increasingly small lattice spacing, but keeping the quantity Na fixed at 25. In each case we made 10^5 Monte Carlo iterations to ensure a good precision. The results can be seen on the table 1.

Table 1: Results for E_0 using 10^5 Monte Carlo iterations, $\overline{n} = 10$ and measurements made every each 5 Monte Carlo iterations

Lattice Spacing a	E_0 Analytical	E_0 Computed	Deviation from theory
5.0×10^{-1}	0.89443	$0.89416 \pm 6.5\times10^{-4}$	2.7000×10^{-4}
2.5×10^{-1}	0.97014	$0.97205 \pm 6.4\times10^{-4}$	-1.9100×10^{-3}
5.0×10^{-2}	0.99875	$1.01907 \pm 6.3\times10^{-4}$	-2.0320×10^{-2}
2.5×10^{-2}	0.99969	$1.02280 \pm 6.4\times10^{-4}$	-2.3110×10^{-2}
5.0×10^{-3}	0.99999	$1.03073 \pm 5.4\times10^{-4}$	-3.0740×10^{-2}

Our estimate for the error is given by

$$\Delta E_0 = \frac{\sigma}{\sqrt{N}}\,, \tag{44}$$

where σ stands for the standard deviation from the data resultant from the Monte Carlo simulation and N is the number of measurements.

The main feature we see in this graph is that the smaller a we get, more we deviate from the analytical value. One possible reason is that our paths are much alike even after 5 entire Monte Carlo iterations when a is small, which violates our work hypothesis for applying our algorithm. To test if that is really the case, we increase the number of Monte Carlo iterations between each measurement for $M = 25$ and test the program with the same set of parameters. To keep the total number of measurements the same (what would affect our error) we increase the number of Monte Carlo simulations to 499600. The results are on the table 2.

Table 2: Results for E_0 using 499600 Monte Carlo iterations, $\overline{n} = 10$ and measurements made every each 25 Monte Carlo iterations

Lattice Spacing a	E_0 Analytical	E_0 Computed	Deviation from theory
5.0×10^{-1}	0.89443	$0.89242 \pm 2.9\times10^{-4}$	2.01×10^{-3}
2.5×10^{-1}	0.97014	$0.96998 \pm 2.8\times10^{-4}$	1.60×10^{-4}
5.0×10^{-2}	0.99875	$0.99963 \pm 2.8\times10^{-4}$	-8.80×10^{-4}
2.5×10^{-2}	0.99969	$0.99546 \pm 2.7\times10^{-4}$	-4.23×10^{-3}
5.0×10^{-3}	0.99999	$1.00418 \pm 3.1\times10^{-4}$	-4.19×10^{-3}

We can see clearly a reduction on error, althought not enough to our computed value and analytical value to agree. Ideally, we should increase the number of simulations between measurements to $M = 50$ in order to obtain a more precise value. However this would require approximatelly one million Monte Carlo iterations to keep fixed the number of measurements. Because of this, it becomes too expensive to make such a simulation.

We proceed to plotting the data from table 2. The idea now is to fit on these data a function and then take the limit $a \to 0$. Since this problem has an analytical solution given by eq. (31), we use it treating the mass m and the parameter μ as free parameters from our fit. Since this method is not general, we try also fit in a polynomial. But from Fig. 3 we see this function approaches the continuum value asymptotically. This means at least its first derivative will be zero at $a = 0$. This hints us an even function and therefore we will include only even powers on the polynomial. At last we try also an ad hoc function $f(a) = A + Ce^{-Ba}$. The fits are shown on Fig. 3 and the resulting parameters on table 3.

Figure 3: Continuum limit analysis for E_0

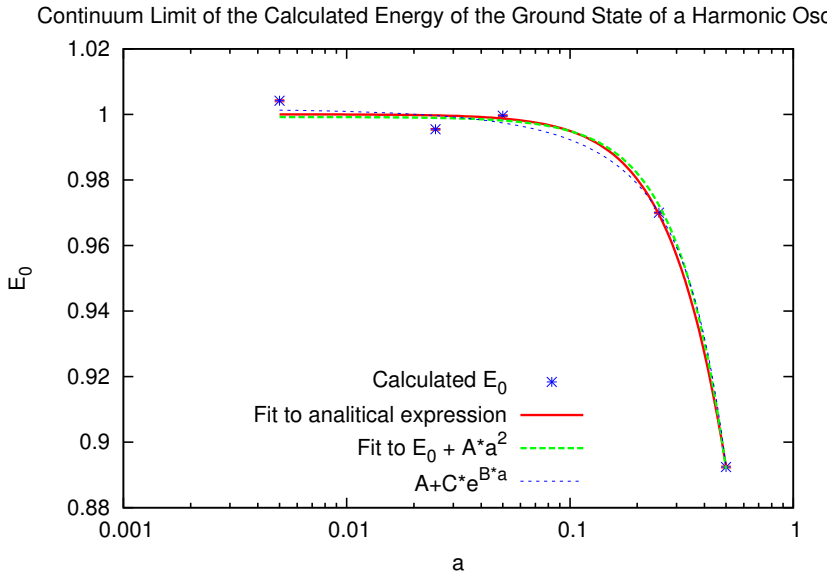

Table 3: Fitting parameters of functions at Fig. 3

$E_0/\sqrt{1+Bx}$	$E_0 + Ax^2$	$A + Ce^{Bx}$ Calculated
$E_0 = 1.000 \pm 0.002$	$E_0 = 0.999 \pm 0.002$	$A = 1.02 \pm 0.01$
$B = 1.02 \pm 0.02$	$A = -0.43 \pm 0.02$	$B = 3.6 \pm 0.8$
		$C = -0.02 \pm 0.01$

The first point to notice is that for larger lattices we have bigger fluctuations than expected by our estimate of the error. This can be again explained by the fact that the paths between measurements are not completely decorrelated for small a. But since these fluctuations are random, our fit converges for the expected value of E_0 [see eq. (31)]. Also we see that the best result is, as expected the fit for the analytical expression. But since this is a special case and the fit to a second order polynomial yielded a good result as well, this will be our prefarable fitting method from now on.

3.2 The Energy of the First Excited State

We want also to predict the energy of the first excited state. As stated on section 1.2, we use two strategies. One is the fit of the correlation function between lattice sites $\Gamma_c^{(2)}$ and the other the direct application of eq. (19). Our program do these calculations automatically and for the same run where we obtained the values at table 2 we have the results of table 4.

Table 4: Results for E_1 using 499600 Monte Carlo iterations, $\overline{n} = 10$ and measurements made every each 25 Monte Carlo iterations

Lattice Spacing a	E_1 Analytical	E_1 Calculated Through Fit	E_1 Calculated Through Eq. (19)
5.0×10^{-1}	2.81928	$2.687 \pm 2.2\times10^{-2}$	$1.94438 \pm 6.4\times10^{-4}$
2.5×10^{-1}	2.94987	$2.863 \pm 1.2\times10^{-2}$	$2.79011 \pm 4.6\times10^{-4}$
5.0×10^{-2}	2.99792	$2.889 \pm 3.7\times10^{-2}$	$2.96684 \pm 5.7\times10^{-4}$
2.5×10^{-2}	2.99948	$2.844 \pm 6.7\times10^{-2}$	$2.96918 \pm 5.6\times10^{-4}$
5.0×10^{-3}	2.99998	$2.228 \pm 4.0\times10^{-1}$	$2.94124 \pm 6.3\times10^{-4}$

We can see clearly these results are not in agreement with the analytical formula. This means the correlation effects affects more the calculation of E_1 than the calculation of E_0. To get better results, we increase the number of Monte Carlo iterations to 999100 paths, but we choose to make a measurement only at each 50 Monte Carlo iterations. With the purpose to make the program run faster, we reduce the parameter $\overline{n}$ to 5. We summarize the results on table 5.

Table 5: Results for E_1 using 999100 Monte Carlo iterations, $\overline{n} = 5$ and measurements made only every 50 Monte Carlo iterations

Lattice Spacing a	E_1 Analytical	E_1 Calculated Through Fit	E_1 Calculated Through Eq. (19)
5.0×10^{-1}	2.81928	$2.8212 \pm 3.8\times10^{-3}$	$2.49800 \pm 5.2\times10^{-4}$
2.5×10^{-1}	2.94987	$2.94069 \pm 9.4\times10^{-4}$	$2.94307 \pm 4.4\times10^{-4}$
5.0×10^{-2}	2.99792	$2.99614 \pm 7.5\times10^{-4}$	$3.00084 \pm 4.1\times10^{-4}$
2.5×10^{-2}	2.99948	$2.99709 \pm 4.4\times10^{-4}$	$2.99732 \pm 4.0\times10^{-4}$
5.0×10^{-3}	2.99998	$2.98905 \pm 2.8\times10^{-2}$	$2.98908 \pm 4.4\times10^{-4}$

We can see that even though we have not achieved a total agreement with the analytical value, we have some more reasonable results. We proceed in taking the continuum limit by the same procedure used for obtaining the value of E_0. Again we see an asymptotic behavior of the points and therefore we use a polinomial $E_1 + Bx^2$.

Table 6: Parameters used for the fit of the graph in Fig. 4

Lattice Spacing a	E_1 Calculated Through Fit	E_1 Calculated Through Eq. (19)
E_1	2.993 ± 0.004	3.01 ± 0.02
A	-0.69 ± 0.03	-2.0 ± 0.17

Figure 4: Continuum limit analysis for E_1 using the two methods described in section 1.2

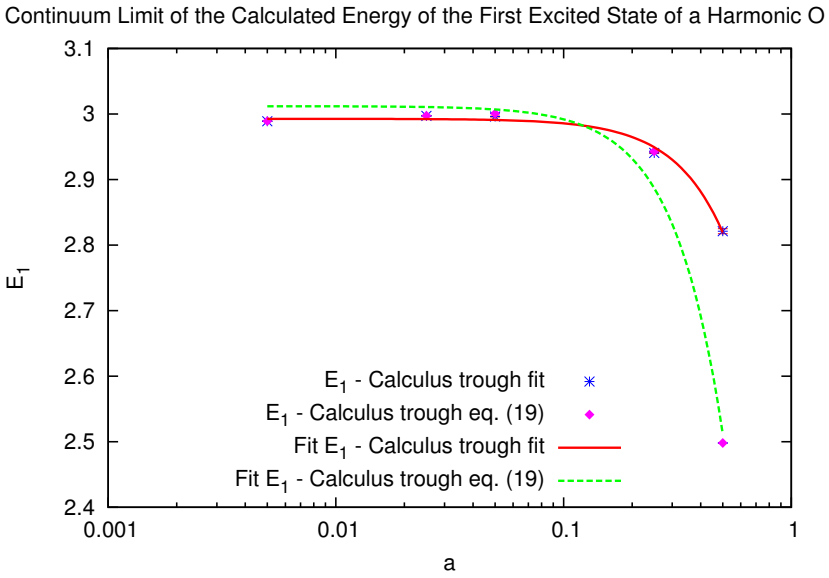

As we can see by the graph in Fig. 4, the point calculated using eq. (19) for $a = 0.5$ completely disagree with the analytical solution. There is two sources of systematical errors that can potentially explain these errors.

The first of them is that according to the theory exposed at section 1.2, the application of the eq. (25) can only be used for $\tau \to \infty$ (large j). We actually do not do this and our j is always setted equal 4. The second source of error comes from the imposition of periodic boundary conditions. Since we impose that $x(\tau_{N+1}) = x(\tau_0)$ it is expected that $\Gamma_c^{(2)}(\tau_{N+1}) = \Gamma_c^{(2)}(\tau_0)$. By the same reason, $\Gamma_c^{(2)}(\tau_N) = \Gamma_c^{(2)}(\tau_1)$ and so on. The effect is that on the plot of $\Gamma_c^{(2)}(\tau)$ instead of a single decaying exponential there is a contribution of a rising exponential as well. The effect of this rising exponential is negligible near the origin, but becomes bigger at large τ originating deviations like the ones that can be seen at Fig. 5 for $\tau = 2.5$. This indicates we needed to find a ballance between these two sources of errors.

On our case, our program keep fixed the value of j at 4 in eq. (25). Since $\tau_j = ja$, keeping j fixed means we are using smaller τ on the calculations and therefore minimizing the effects of the errors due the influence of boundary conditions. The cost of that is an increase on errors due escaping our working hypothesis conditions. However since the errors coming from the use of eq. (25) usually get smaller for smaller a we can say the effects of the boundary conditions are far superior. We must highlight however this analysis is just an qualitative approach. These errors should be carefully analysed in a quantitative way. This analysis should also include also the propaagation of the errors of E_0 on the calculation of E_1, since on all cases we calculate just the difference $E_1 - E_0$ and then adds E_0 to the result. We do not do these analysis here however due time constraints.

Figure 5: $\langle x(0)x(\tau)\rangle$ as function of τ for $a = 0.5$

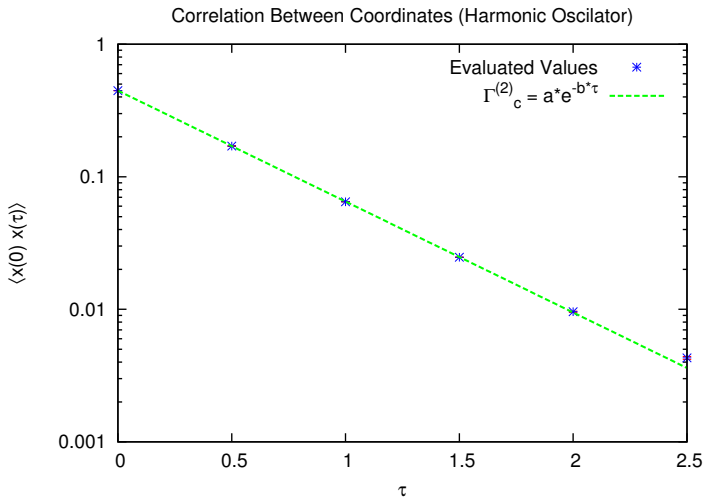

We turn our attention again on the analysis of Fig. 4 and the parameters of Table 6. We can observe that the value of E_1 for the case where the fit was made using the values of E_1 obtained through eqhese calculation were all done with the mass set equal unity. (19) do not agree with the analytical value of $E_1 = 3$, which is expected given our explanation of why this method is giving worst results. However, we reach agreement with the analytical solution using the method where we fit our data at eq. (18).

4 Conclusions

During our stay here at DESY Zeuthen we studied the path integral formulation of non-relativistic quantum mechanics. As it was presented in the report, we used the Metropolis algorithm to make this calculation for the harmonic oscillator, which has an analytical solution and thus comparrison with theoretical results was possible.

At the begining we spent a long time learning about theoretical aspects of the problem, relying on references [3] and [2]. When we accomplished theoretical researches and got familiar with the path integral and lattice approach to quantum mechanics, we started to deal with computational tasks concerning the harmonic oscillator. A significant part of the time was spent coding, performing the simulations and data analysis. Every time we had some doubts, we consulted our supervisors to have a clear idea about the next steps.

For the implementation of the algorithm we wrote programs using the FORTRAN programming language. For plots and data analysis we used GNUPLOT program. The numerical Monte Carlo method was adopted for the example of E_0 and E_1 calculations, which gave us insight into topics of thermalization and correlation effects. We could observe how numerical simulations behave due to changes in the input parameters and how the quantum mechanics paths evolve in time. In particular, we studied how the discretized quantum mechanical system approaches the continuum limit. For this we performed simullations at smaller and smaller lattice spacings, keeping the physical time constant.

Our final results are compatible with the analytical values. Thus we can conclude our code has been verified and works properly. As discussed in the report, there appeared some

systematic errors, which we cannot discuss here because of lack of time to analyze them. Nonetheless, the computation we have made for the harmonic oscillator can be repeated and used for other potentials, such as the anharmonic oscillator.Therefore, what we have accomplished in the DESY Zeuthen Summer Student Programme can serve as a basis for future investigations of quantum mechanical systems in the path integral formulation.

Acknowledgements

First of all, we would like to thank our great supervisor Karl Jansen for leading us in this project, for his endless patience and all effort he put to the DESY Summer Student Programme this year. Secondly, we thank Andreas Nube and Andreas Athenodorou for taking care of us and giving always exhausting answers for all our questions. We are very gratefull for the help and support received from the PhD students we shared office with: Elena Garcia Ramos, Attila Nagy and Pan Kessel. Moreover, we would like to thank all others members of the NIC group who created an unique atmosphere during our stay here (we **really loved** NIC's songs!) and therefore made it a pleasure for us to work as a part of the NIC group. During the time we spent here, we gained exceptional experience and met amazing people. Finally, we would like to thank others summer students who took part in this program for extraordinary lovely summer time we could spend here together! Undoubtedly, it was an honour for us to participate in DESY Summer Students Programme this year.

Appendixes

A Derivation of the kernel for a free particle

On these appendixes we will derive the kernel [$K(b,a) = \langle b|e^{-iHt}|a\rangle$ - see eq. (6)] for the harmonic oscillator. First for illustration of our method we do this calculation for the simpler case of an one dimensional free particle, which has the Lagraangian

$$L[\dot{x}, x, t] = \frac{m}{2}\dot{x}^2 \,. \tag{45}$$

We assume

$$x(t) = \bar{x}(t) + y(t) \,, \tag{46}$$

where $\bar{x}(t)$ is a classical path and $y(t)$ stands for the difference between the classical path $\bar{x}(t)$ and a given path $x(t)$ (see Figure 6).

We use eq. (46) and the Lagrangian given in 45 to write the action as

$$\begin{aligned} S[x(t)] &= \int_{t_a}^{t_b} \left[\frac{m}{2}\dot{\bar{x}}^2 + \frac{m}{2}\dot{y}^2 + \frac{m}{2}\dot{\bar{x}}\dot{y}\right] \, dt \\ &= S_{cl} + S[y(t)] + \frac{m}{2}\int_{t_a}^{t_b} \dot{\bar{x}}\dot{y} \, dt \,. \end{aligned} \tag{47}$$

It can be shown that (see Appendix C)

$$\frac{m}{2}\int_{t_a}^{t_b} \dot{\bar{x}}\dot{y} \, dt = 0 \,, \tag{48}$$

Figure 6: An arbitrary path may be written as the classical path $\bar{x}(t)$ plus a fluctuation $y(t)$ around it.

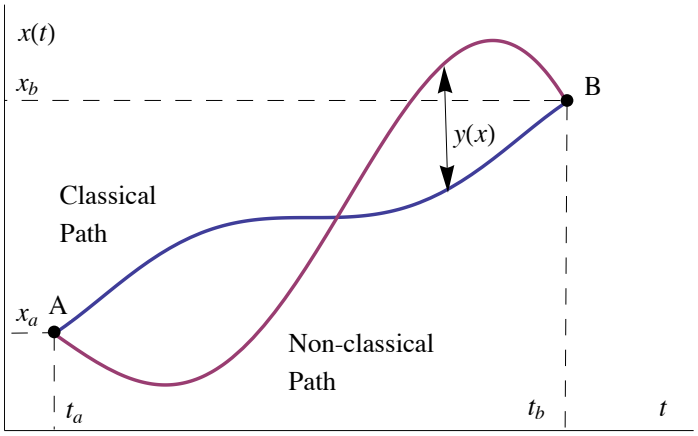

and therefore

$$S[x(t)] = S_{cl} + S[y(t)]\,. \tag{49}$$

Then we can compute eq. (6) as

$$K(b,a) = \int_{t_a}^{t_b} \mathcal{D}[x(t)]\; e^{\frac{i}{\hbar}S[x(t)]} = e^{\frac{i}{\hbar}S_{cl}} \int_{t_a}^{t_b} \mathcal{D}[x(t)]\; e^{\frac{i}{\hbar}S[y(t)]}\,. \tag{50}$$

Since the end points are fixed, $y(t_a) = y(t_b) = 0$ and therefore $y(t)$ has a period $T = t_b - t_a$. Considering a Fourier transform for $y(t)$, we derive

$$y(t) = \sum_{n=-\infty}^{\infty} a_n \sin\left(\frac{n\pi t}{T}\right), \tag{51}$$

$$\dot{y}^2 = \sum_{n=-\infty}^{\infty}\sum_{k=-\infty}^{\infty} a_n a_k \frac{nk\pi^2}{T^2} \cos\left(\frac{n\pi t}{T}\right)\cos\left(\frac{k\pi t}{T}\right). \tag{52}$$

When integrating eq. (52) over the period, the sum on k will be only non-zero for $n = k$, when it yelds $T/2$. Therefore the integral is given by

$$\int \dot{y}^2\, dt = \sum_{n=-\infty}^{\infty} a_n^2 \frac{n^2\pi^2}{T^2}\frac{T}{2} = \sum_{n=-\infty}^{\infty} a_n^2 \frac{n^2\pi^2}{2T^2}\,. \tag{53}$$

Wherefore, kernel for the system can be rewritten as

$$K(b,a) = e^{\frac{i}{\hbar}S_{cl}} \int_{-\infty}^{\infty} \prod_{i=1}^{\infty} e^{\frac{im}{2\hbar}a_n^2 \frac{n^2\pi^2}{2T^2}} \mathcal{D}[(y(t)]\,. \tag{54}$$

Substituting ω_n for $\frac{n\pi}{T}$ we transform $y(t)$ expression 51 to

$$y(t_i) = \sum_{i=1}^{N-1} a(\omega_n)\sin(\omega_n t_i)\,. \tag{55}$$

Then,

$$\frac{\partial y(t_i)}{\partial a(w_k)} = \sum_{i=1}^{N-1} \delta_{kn} \sin(w_n t_i) = \sin(w_k t_i)\,. \tag{56}$$

The jacobian J of the transformation is given by a constant value. Using all derived results we express kernel as

$$K(b,a) = \left[\lim_{\epsilon\to 0}\lim_{N\to\infty} A \int_{-\infty}^{\infty}\cdots\int_{-\infty}^{\infty} \prod_{n=1}^{N} e^{\frac{im}{2\hbar}\cdot\frac{a_n^2 n^2\pi^2}{2T}}\, da_1\cdots da_{N-1}\right] e^{\frac{i}{\hbar}S_{cl}}\,. \tag{57}$$

After integrating, we finally obtain

$$K(b,a) = \lim_{\epsilon\to 0}\lim_{N\to\infty} A \prod_{n=1}^{N} \sqrt{\frac{4i\hbar T}{n^2\pi^2 m}}\, e^{\frac{i}{\hbar}S_{cl}}\,, \tag{58}$$

and therefore

$$K(b,a) = \lim_{\epsilon\to 0}\lim_{N\to\infty} \bar{A}\, e^{\frac{im}{2\hbar T}(x_b - x_a)^2}\,, \tag{59}$$

since the productory of the square root above is just a constant on the limit $N\to\infty$ and $\bar{A}$ in eq. (59) stands for the normalization constant in the kernel expression. It may be choosed in a way that once the limit is evaluated, the kernel will result on the one obtained on [3, pg. 42]

$$K(b,a) = \sqrt{\frac{2\pi i\hbar T}{m}} \exp\left[\frac{im(x_b - x_a)^2}{2\hbar T}\right]\,. \tag{60}$$

B The Kernel For The Harmonic Oscillator

We will now use the same procedure to evaluate the kernel for the harmonic oscillator problem. Its Lagrangian is given by

$$L[\dot{x}, x, t] = \frac{m\dot{x}^2}{2} - \frac{m\omega^2 x^2}{2}\,. \tag{61}$$

We use the same procedure of considering fluctuations around the classical path to describe any given path. The Lagrangian becomes

$$L[\dot{y}, y, t] = \frac{m\dot{\bar{x}}^2}{2} - \frac{m\omega^2\bar{x}^2}{2} + \frac{m\dot{y}^2}{2} - \frac{m\omega^2 y^2}{2} + m\dot{\bar{x}}\dot{y} - m\omega^2\bar{x}y\,. \tag{62}$$

The same reasoning as before is used to conclude that $y(t)$ is periodic with period $T = t_b - t_a$ and therefore may be expanded as a fourier series

$$y(t) = \sum_{n=1}^{N-1} a(\omega_n)\sin(\omega_n t)\,. \tag{63}$$

Where $\omega_n = n\pi/T$. Notice that there is no cossine term on this series. This is because we may choose without losing generality $t_a = 0$ and $t_b = T$. Since we know that $y(0) = 0$, if we set all the coeficients accompanying the cossines to 0, we automatically meet this condition.

From classical mechanics we write the classical path

$$\bar{x}(t) = A\cos(\omega t + \varphi)\,. \tag{64}$$

We then substitue eq. (64) and eq. (63) into eq. (62) and integrate the result on time from 0 until T to obtain the action through this path. The end result will be

$$\begin{aligned} S = S_{Cl} + \sum_{n=1}^{N-1} m \left\{ a\left(\omega_n\right) \frac{\sqrt{T\left(\omega_n^2 - \omega^2\right)}}{2} - \frac{A\omega\left[\cos(\omega T + \varphi)(-1)^n - 1\right]}{\sqrt{T\left(\omega_n^2 - \omega^2\right)}} \right\}^2 \\ - \frac{A^2\omega^2\left[\cos(\omega T + \varphi)(-1)^n - 1\right]^2}{T\left(\omega_n^2 - \omega^2\right)}\,. \end{aligned} \tag{65}$$

Here it was used the orthogonality relationship between the functions $\sin\left(\omega_n t\right)$ and $\sin\left(\omega_k t\right)$ as well between $\cos\left(\omega_n t\right)$ and $\cos\left(\omega_k t\right)$

$$\int_0^T \sin\left(\omega_n t\right)\sin\left(\omega_k t\right) dt = \int_0^T \cos\left(\omega_n t\right)\cos\left(\omega_k t\right) dt = \delta_{nk}\frac{T}{2}\,, \tag{66}$$

and the result is adjusted to eq. (65) by completing squares. Note that our integral over an arbitrary path, was changed to the integral over the fluctuations around the classical path. Therefore when we calculate $e^{iS/\hbar}$ the term containing the classical action will be seen as a constant to the integral. Also, when we considered to describe the fluctuations as a fourier series, our variable changed again to the fourier series coeficients. We need then to relate these two integral variables. This is done by discretising the time in a lattice with spacing ε in such way that $N\varepsilon = T$. This way we estabilish the relationship

$$\begin{aligned} \mathcal{D}\left[y(t)\right] &= \lim_{N\to\infty} B(N,\varepsilon) \prod_{i=1}^{N-1} dy(t_i) \\ &= \lim_{N\to\infty} B(N,\varepsilon) \left|\frac{\partial\left[y(t_1), y(t_2), \cdots, y(t_{N-1})\right]}{\partial\left[a(\omega_1), a(\omega_1), \cdots, a(\omega_{N-1})\right]}\right| \prod_{i=1}^{N-1} da(\omega_i)\,. \end{aligned} \tag{67}$$

The factor that accompanies the differentials of the fourier coefficients is the Jacobian and it is easy to show using the Jacobian definition and eq. (63) that it independs of $a(\omega_i)$ and therefore it is treated as a constant. $B(N,\varepsilon)$ is a normalization constant that needs to be determined. The kernel will be then

$$\begin{aligned} K(b,a) = \lim_{N\to\infty} B(N,\varepsilon) J \prod_{i=1}^{N-1} \exp\left[\frac{i}{\hbar} S_{cl}\right] \exp\left\{-\frac{iA^2\omega^2\left[\cos(\omega T + \varphi)(-1)^n - 1\right]^2}{\hbar T\left(\omega_n^2 - \omega^2\right)}\right\} \\ \int_{-\infty}^{\infty} \exp\left[\frac{im}{\hbar}\left\{ a\left(\omega_n\right)\frac{\sqrt{T\left(\omega_n^2 - \omega^2\right)}}{2} - \frac{A\omega\left[\cos(\omega T + \varphi)(-1)^n - 1\right]}{\sqrt{T\left(\omega_n^2 - \omega^2\right)}}\right\}^2\right] da(\omega_n)\,. \end{aligned} \tag{68}$$

This is a Gaussian integral, which can be easily evaluated to

$$\begin{aligned} K(b,a) = \lim_{N\to\infty} B(N,\varepsilon) J \exp\left[\frac{i}{\hbar} S_{cl}\right] \\ \prod_{i=1}^{N-1} \exp\left\{-\frac{iA^2\omega^2\left[\cos(\omega T + \varphi)(-1)^n - 1\right]^2}{\hbar T\left(\omega_n^2 - \omega^2\right)}\right\} \sqrt{\frac{4i\hbar}{mT\left(\omega_n^2 - \omega^2\right)}}\,. \end{aligned} \tag{69}$$

We can rewrite this as

$$K(b,a) = \lim_{N\to\infty} B(N,\varepsilon) J \exp\left[\frac{i}{\hbar} S_{cl}\right] \left(\frac{4i\hbar}{mT}\right)^{(N-1)/2} \prod_{i=1}^{N-1} \left(\frac{n^2\pi^2}{T^2}\right)^{-1/2} \prod_{i=1}^{N-1} \exp\left\{-\frac{iA^2\omega^2\left[\cos(\omega T+\varphi)(-1)^n-1\right]^2}{\hbar T\left(\omega_n^2-\omega^2\right)}\right\} \prod_{i=1}^{N-1}\left(1-\frac{T^2\omega^2}{n^2\pi^2}\right)^{-1/2}. \tag{70}$$

We can use now the property exposed in [3, pg. 73]

$$\lim_{N\to\infty} \prod_{i=1}^{N-1}\left(1-\frac{T^2\omega^2}{n^2\pi^2}\right)^{-1/2} = \sqrt{\frac{\omega T}{\sin(\omega T)}} \tag{71}$$

and the classical action for the harmonic oscillator [3, pg. 28] (see Appendix E)

$$S_{Cl} = \frac{m\omega}{2\sin(\omega T)}\left[(x_a^2+xb^2)\cos(\omega T) - 2x_a x_b\right] \tag{72}$$

to arrive at the final expression

$$K(b,a) = C\exp\left\{\frac{im\omega}{2\hbar\sin(\omega T)}\left[(x_a^2+xb^2)\cos(\omega T) - 2x_a x_b\right]\right\}\sqrt{\frac{\omega T}{\sin(\omega T)}}, \tag{73}$$

where C is a normalization constant and it is the result of all the remaining factors collected together and on the limit of $N\to\infty$. We can recover it noticing that on the limit of zero frequency, we should recover the free particle. By this procedure we can see that

$$C = \sqrt{\frac{m}{2\pi i\hbar T}} \tag{74}$$

and therefore

$$K(b,a) = \sqrt{\frac{m\omega}{2\pi i\hbar\sin(\omega T)}}\exp\left\{\frac{im\omega}{2\hbar\sin(\omega T)}\left[(x_a^2+xb^2)\cos(\omega T) - 2x_a x_b\right]\right\}. \tag{75}$$

C Calculation of the integral of the crossed term in the free particle action

Considering

$$\bar{x}(t) = \bar{x_0} + \dot{\bar{x}}t, \tag{76}$$

where

$$\dot{\bar{x}} = \frac{x_b - x_a}{t_b - t_a}, \tag{77}$$

the last expression in eq. (47) change to

$$\frac{m}{2}\int_{t_a}^{t_b} \dot{\bar{x}}\dot{y}\ dt = \frac{m\dot{\bar{x}}}{2}\int_{t_a}^{t_b}\dot{y}\ dt\,. \tag{78}$$

Substituting the Fourier tramsform to $\dot{y}$ in eq. (51), integral above becomes zero

$$\int_0^T \dot{y}\ dt = \int_0^T \sum_{n=1}^{n=N} a_n \omega_n \cos(\omega_n t)\ dt = 0\,. \tag{79}$$

D Classical action for the free particle

We know that Lagrangian L for the free particle is equal to

$$L[\dot{x}, x, t] = \frac{m}{2}\dot{x}^2\,. \tag{80}$$

The action S is given by the expression

$$S = \int_{t_a}^{t_b} L(\dot{x}, x, t)\ dt\,. \tag{81}$$

Using the Lagrange's equation

$$\frac{d}{dt}\frac{\partial L}{\partial \dot{x}} - \frac{\partial L}{\partial x} = 0\,, \tag{82}$$

we will derive an expression for the classical action corresponding to the classical motion of a free particle. Substituting Lagrangian given in eq. (80 into eq. (82), we get

$$\begin{aligned} &\frac{d}{dt}\frac{\partial L}{\partial \dot{x}} - \frac{\partial L}{\partial x} = \frac{m}{2}\frac{d}{dt}\dot{x} - 0 = 0, \\ &\frac{d}{dt}\dot{x} = 0 \implies \dot{x} = constant\,. \end{aligned} \tag{83}$$

Therefore

$$S_{cl} = \int_{t_a}^{t_b} \frac{m}{2}\dot{x}^2\ dt = \frac{m}{2}\dot{x}^2 \int_{t_a}^{t_b} dt = \frac{m}{2}\dot{x}^2(t_b - t_a)\,. \tag{84}$$

Since $\dot{x}$ is time independent, it can be expressed as

$$\dot{x} = \frac{x_b - x_a}{t_b - t_a}\,. \tag{85}$$

Finally, the classical action is

$$S_{cl} = \frac{m}{2}\frac{(x_b - x_a)^2}{t_b - t_a}\,. \tag{86}$$

E Classical Action for The Harmonic Oscillator

The Lagrangian for the Harmonic Oscillator is given by eq. (61). Using eq. (82) we arrive at the differential equation

$$\ddot{x} + \omega^2 x = 0\,. \tag{87}$$

The solution for this equation is widely known to be eq. (64). We also impose the initial conditions

$$\begin{aligned} x_a &= \cos(\omega t_a + \varphi) \\ x_b &= \cos(\omega t_b + \varphi)\,. \end{aligned} \tag{88}$$

We then substitute eq. (64) into eq. (61) and integrate on time from t_a to t_b to obtain the classical action. The obtained result will be

$$S_{Cl} = \frac{m\omega A^2}{2}\left[\sin(\omega t_b + \phi)\cos(\omega t_b + \phi) - \sin(\omega t_a + \phi)\cos(\omega t_a + \phi)\right]\,. \tag{89}$$

We use then that $t_b = T + t_a$ and eq. (88) to rearrange the above equation, arriving at the expression exposed on [3, pg.28] and written on eq. (72).

References

[1] A. Zee, *Quantum Field Theory in a Nutshell*, Second Edition, (Princeton University Press,2010)

[2] M. Creutz and B. Freedman, *A Statistical Approach to Quantum Mechanics*, Annals of Physics, **132**, 427-462 (1981).

[3] Feynman, R. P., and Hibbs, A. R., *Quantum Mechanics and Path Integrals*, New York: McGraw-Hill, 1965

[4] GNUPLOT tips - not so frequently asked questions, 30 August 2012 [online]. Available from: <http://t16web.lanl.gov/Kawano/gnuplot/index-e.html>

[5] Clive G. Page, Professional Programmer's Guide to Fortran77, 30 August 2012 [online]. Available from: <http://www.star.le.ac.uk/ cgp/prof77.html>

[6] C. K. Shene, Fortran 90 Tutorial, 30 August 2012 [online]. Available from: <http://www.cs.mtu.edu/ shene/COURSES/cs201/NOTES/fortran.html>

[7] A. Nube, private communication.